Photophysical studies of amorphous orientation in poly(ethylene terephthalate) films

David J. Hemker and Curtis W. Frank*
Department of Chemical Engineering, Stanford University, Stanford, CA 94305-5025, USA

and Jule W. Thomas
E. I. Du Pont de Nemours & Company, Brevard, NC 28712, USA
(Received 29 July 1987; accepted 2 October 1987)

The effects of uniaxial and biaxial extension on the intrinsic fluorescence of poly(ethylene terephthalate) (PET) films have been investigated. A power law relationship, valid for both uniaxially and biaxially deformed samples, was found between the fluorescence emission at 368 nm and the planar extension, which is defined as the product of the extension ratios in the transverse and machine directions. Dimethyl terephthalate (DMT) model compound studies indicate that the fluorescent species in the PET films is not the monomeric unit. The dependence of emission intensity at 368 nm on orientation was greater when the films were excited with 300 nm light than with 340 nm. However, the absolute emission intensity was an order of magnitude larger when the excitation wavelength was 340 nm as compared to 300 nm. Transient fluorescence measurements show that the 368 nm emission has an average lifetime of 1.3 ns when using 340 nm excitation, and an average lifetime of 3.8 ns when exciting at 300 nm. A model incorporating energy migration in the non-crystalline region has been proposed to explain these results.

(Keywords: poly(ethylene terephthalate); orientation; fluorescence spectroscopy)

INTRODUCTION

Poly(ethylene terephthalate) (PET) is used extensively in the fibre and packaging industries. Since, in general, orientation in a polymeric fibre or film greatly influences mechanical properties such as tensile strength, numerous studies have investigated the effects of orientation on the physical and microscopic properties of PET in the solid state[1-7]. Fluorescence spectroscopy has often been used to probe molecular orientation in these systems. However, these investigations have generally employed small-molecule chromophores added to the melt as fluorescent sensors[8-12] and have generally used polarized fluorescence techniques.

As an example of such an extrinsic probe study, Nobbs *et al.* used polarized fluorescence to study uniaxially drawn PET tapes in which molecules of 4,4'-(dibenzoxazolyl)stilbene were dispersed[10-12]. They showed that in both amorphous and semicrystalline samples the results from the fluorescence of oriented probe molecules agreed with the results of optical birefringence. It was also learned that the probe molecules were preferentially located in the amorphous regions of the polymer.

These conclusions and the infra-red results of Cunningham *et al.*[13] led to a model in which it was proposed that the orientation of PET at 353 K takes place primarily via the deformation of a rubber-like affine network with about six equivalent freely jointed random links between crosslink points[10,13]. The crosslink points were postulated to be chain entanglements. Data were found to be in agreement with the model up to draw ratios of about 3.5.

The intrinsic fluorescence of PET has been less well characterized[14-17]. The structures of PET and its corresponding model compound, dimethyl terephthalate (DMT), are shown below.

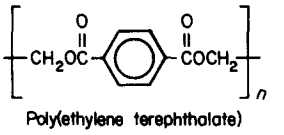

Poly(ethylene terephthalate)

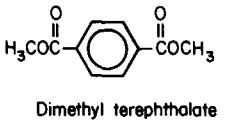

Dimethyl terephthalate

It is important to note that the aromatic ring in the chain backbone makes PET a feasible candidate for intrinsic fluorescence studies. Depending upon the geometry, this structure could conceivably give rise to both monomer and excimer fluorescence as well as energy migration among rings. Moreover, the carbonyl groups adjacent to the backbone ring could lead to interactions that might result in exciplex formation. Since the ring is incorporated into the molecule via the chain backbone, fluorescence from the ring could provide more accurate information about the chain backbone orientation than if small-molecule dopant chromophores were used.

In photophysical terms, the interactions between the carbonyl groups and the aromatic ring make PET a much more complex system than, for example, polystyrene.

* To whom correspondence should be addressed.

0032-3861/88/030437-11$03.00

Phillips *et al.*[14] suggested than an emission at 370 nm originates from either the triplet state or a tightly bound excimer. In fact, a peak at 375 nm has been attributed to a PET excimer by Takai *et al.*[16]. However, Allen and McKellar[17] contend that a 392 nm peak is from an associated ground state dimer. More evidence for a ground state dimer was provided recently by Hennecke and Fuhrmann, who used polarized fluorescence to show that the emission anisotropy in the 385 nm region was independent of excitation wavelength[18]. The anisotropy was also found to be near the theoretical limit for an isotropic system.

Hennecke *et al.* have also studied intrinsic PET emission for uniaxially oriented films using polarized fluorescence[19]. They found that the orientation of semicrystalline PET could be approximated by a superposition of the affine network model and a vector-affine model. The vector-affine model describes the preferred orientation of rigid rods or ellipsoids in an affinely deformed matrix. In the same study they also found that the intrinsic fluorescence of PET films increased for uniaxial extension ratios between 2 and 5.

Fewer studies have focused on the effects of biaxial orientation in PET films[20–22]. Early work by Heffelfinger and Schmidt employed X-ray diffraction and infra-red measurements to study uniaxially and biaxially deformed films of semicrystalline PET[21]. Their results gave insight into the morphological changes that occur during uniaxial and biaxial stretching. They found that uniaxial orientation forced some of the PET repeat units existing in a *gauche* conformation to be converted into the more extended *trans* conformation. For stretch ratios less than about 3.5, the newly formed *trans* structure was incorporated into both the amorphous and crystalline regions in about equal amounts. This means that there was both alignment in the amorphous regions and crystallite growth. For non heat-set, biaxially oriented samples with machine direction × transverse direction stretch ratios ranging from 2.0 × 3.5 to 3.5 × 3.5, they found that all of the increase in *trans* content due to orientation was taken up in the amorphous regions.

In order to apply intrinsic photophysical methods to the study of molecular orientation in semicrystalline PET, we have proceeded with the following approach. Our overall goal is to use non-polarized fluorescence methods, instead of more complicated polarized fluorescence techniques, to gain an understanding of orientation effects. A more specific objective is concerned with investigating the effects of uniaxial and biaxial orientation in PET films, such as those proposed in earlier models, using the intrinsic fluorescence of the polymer as the probe. A secondary goal is to obtain a better understanding of the structure of the intrinsic fluorescent species in PET.

EXPERIMENTAL

Film preparation

Nine films of PET were prepared in various states of uniaxial and biaxial deformation. After deformation, the thickness of the samples ranged from 0.02 to 0.7 mm. The biaxial stretching was accomplished by heating the sample to 368 K and then simultaneously extending the sample in the machine and transverse directions. This should allow relatively easy rearrangement of the disordered amorphous regions since the glass transition temperature of the material, measured by differential scanning calorimetry (d.s.c.), is 353 K. The important parameter reflecting the mechanical deformation history of the film is the extension ratio, defined as the ratio of sample length after stretching to sample length prior to stretching. The extension ratios in the machine and transverse directions for each sample are shown in *Table 1*.

The DMT model compound was obtained from Aldrich Chemical Company in crystalline form. Methanol, dichloromethane, hexane, trifluoroacetic acid (TFAA) and dichloroacetic acid (DCAA) were also obtained from Aldrich.

Film extractions were done using a Soxhlet extraction apparatus employing methanol, dichloromethane and hexane as solvents. All extractions were carried out for a minimum of 48 h at the solvent reflux temperature.

Fluorescence measurements

Fluorescence experiments were carried out using a SPEX Fluorolog 212 spectrometer employing a 450 watt xenon source. All measurements were made using a band pass of 4 nm and front face illumination. All spectra were corrected for the spectral response of the instrumentation. Excitation wavelengths of 260 to 380 nm and emission wavelengths of 270 to 550 nm were investigated.

Fluorescence lifetime measurements

Transient fluorescent lifetime measurements were performed on a Photochemical Research Associates, PRA 3000, nanosecond time-correlated single photon counting spectrometer. The instrument uses a standard configuration consisting of a thyratron-gated, hydrogen-filled flash lamp as the excitation source, Jobin–Yvon excitation and emission monochromators, Hamamatsu R928 Peltier cooled photomultiplier, and Ortec single photon counting electronics. The monochromator band pass for all measurements was 10 nm. Data were stored on a Tracor Northern TN1750 multichannel analyser and transmitted to a DEC 11/23 minicomputer for analysis.

A typical lifetime spectrum consisted of 30 000 counts at the peak channel. The rate of data collection was kept below 2% of the excitation repetition rate to eliminate multiphoton interference. A lamp profile for each film sample was obtained by measuring the scattered light from the sample with both the excitation and emission monochromators set to the excitation wavelength to be used in the experiment. In order to minimize any longterm time drift or change in lamp pulse shape, lamp

Table 1 Orientation of PET films studied

Sample no.	Extension ratios		
	Machine direction	Transverse direction	Planar extension
1	1	1	1
2	2	1	2
3	3	1	3
4	3	3	9
5	3.5	1	3.5
6	3.5	3.5	12.25
7	4	1	4
8	4	4	16
9	2	2	4

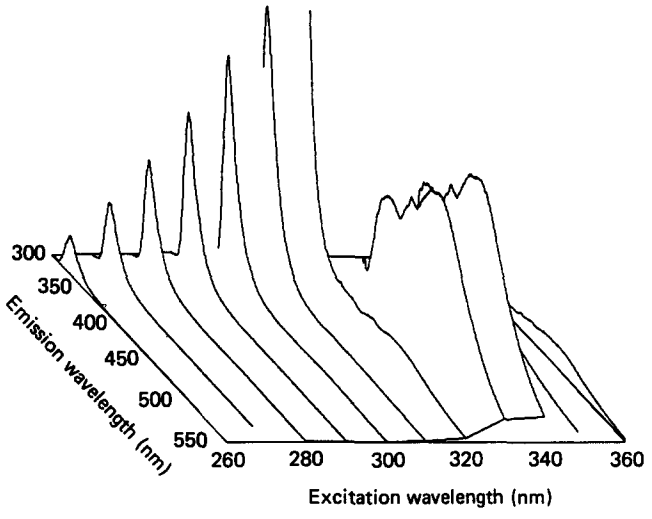

Figure 1 Fluorescence characterization of DMT crystals

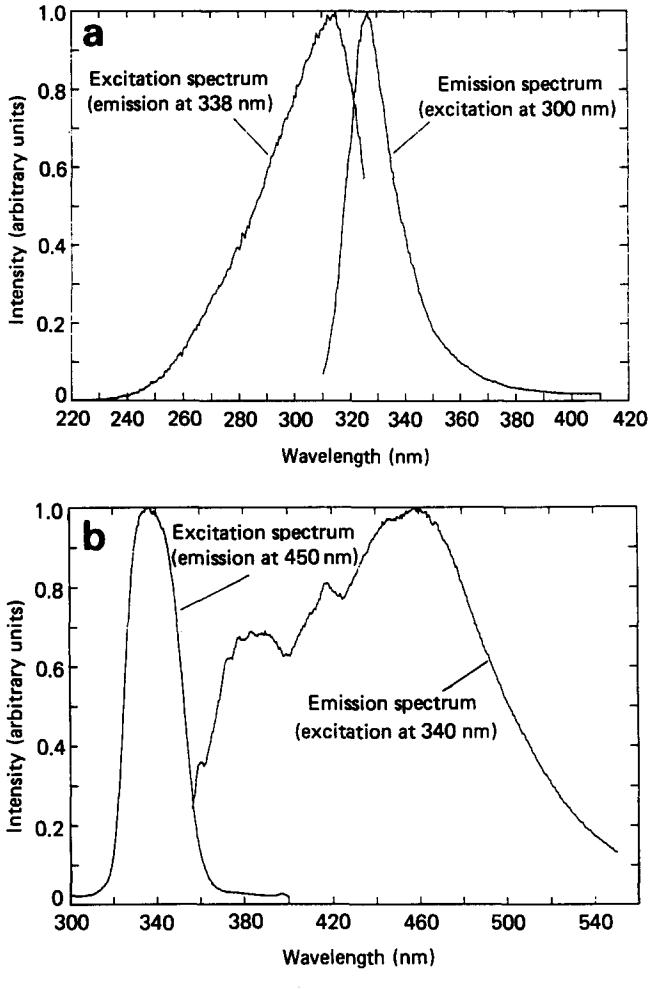

Figure 2 (a) Fluorescence excitation and emission spectra of DMT crystals in the low excitation wavelength region. (b) Fluorescence excitation and emission spectra of DMT crystals in the high excitation wavelength region

profiles at the start and end of each experiment were averaged.

The fluorescence decay profiles were fitted to the model trial function using a non-linear χ^2 minimization algorithm of Marquardt. Several goodness-of-fit statistical parameters, including reduced χ^2, weighted residuals, autocorrelation function, Durbin–Watson parameter, runs test and correlation coefficients, were analysed for each run. The photomultiplier used in this system exhibited a relatively small wavelength dependence in the range of interest. Therefore, no corrections for the energy-dependent time shift of the photomultiplier were required.

Differential scanning calorimetry

D.s.c. measurements were performed on a Perkin-Elmer DSC-II. The instrument was calibrated to within ± 0.5 K using indium and lead standards. All data were taken using a scan rate of 20 K min^{-1}.

RESULTS

Photostationary fluorescence

In order to determine the feasibility of using intrinsic PET fluorescence and to aid in selecting appropriate excitation wavelengths, fluorescence characterizations of the DMT model compound and an unoriented PET film were performed. This was accomplished by first setting the excitation wavelength and then scanning the emission spectrum. The excitation wavelength was then increased by 10 nm and the sample was rescanned. This process was repeated for a number of excitation wavelengths.

The fluorescence spectra of the DMT crystals examined in this fashion and given in *Figure 1* show that the emission depends upon the excitation wavelength. A sharp, narrow emission peak is observed for excitations below 320 nm and two broad emission bands are found when excitation above 320 nm is used. An anomalous peak at 417 nm, in this and subsequent spectra, was caused by a defect in the monochromator at this wavelength. This emission, however, does not affect any analysis given below. *Figure 2* gives more detailed representative excitation and emission spectra for DMT crystals for the two regions. In *Figure 2a*, the emission intensity maximum at about 327 nm results from an excitation at 300 nm. Thus, in PET the monomer unit should be excited by light of 320 nm or less. However, when exciting with 340 nm light, a peak at 390 nm and a broad emission at 460 nm are observed, as shown in *Figure 2b*.

A comparable three-dimensional plot of the fluorescence behaviour for the unoriented PET film is shown in *Figure 3*. Although there is a strong dependence

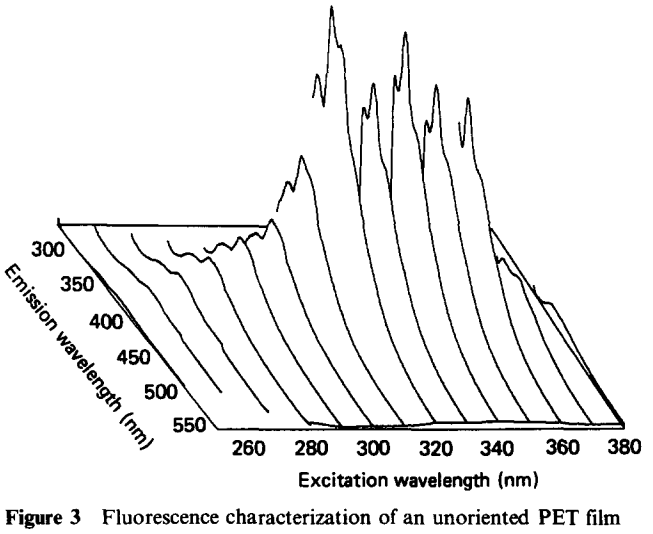

Figure 3 Fluorescence characterization of an unoriented PET film

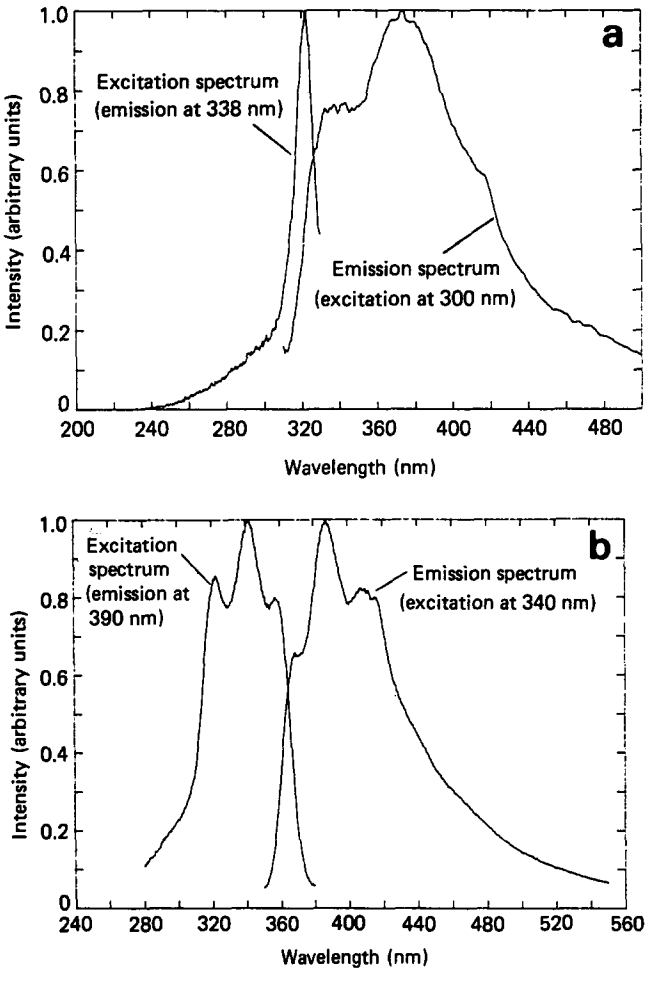

Figure 4 (a) Fluorescence excitation and emission spectra for an unoriented PET film in the low excitation wavelength region. (b) Fluorescence excitation and emission spectra for an unoriented PET film in the high excitation wavelength region

of emission intensity on excitation wavelength for unoriented PET films, the spectra for excitation less than 310 nm are similar in structure but much less well resolved than for higher excitation wavelengths. The fluorescence characterization shows that an overall emission maximum at 386 nm is obtained when the film is excited at 340 nm. The corresponding excitation and emission spectra for an unoriented film are given in *Figure 4*. When excited with 300 nm light, the film emission spectrum has peaks at 338 and 368 nm, as shown in *Figure 4a*. The excitation spectrum of the 338 nm emission peak is sharp, with a maximum at 322 nm. *Figure 4b* shows that peaks in the excitation spectrum of an unoriented PET film for emission at 390 nm, however, occur at 321, 341 and 357 nm, with a slight shoulder at about 295 nm. Emission peaks for excitation at 340 nm occur at 368 and 386 nm, with a shoulder at 410 nm.

Fluorescence spectra of each of the oriented films were taken using excitation wavelengths of 300 and 340 nm. The model compound characterization showed that 300 nm light should excite the monomer unit of PET. The 340 nm excitation wavelength was chosen because that excitation energy produced the strongest emission from PET. The dependence of the intensity of the 368 nm peak on orientation, normalized with respect to thickness, is plotted in *Figure 5* for each excitation wavelength. The 368 nm peak was chosen since it is clearly discernible in the emission spectra resulting from both excitation wavelengths. Planar extension was selected as the parameter used to characterize orientation[20]. A least-squares line is drawn through each set of data. Note that 340 nm excitation produced an emission intensity that is almost an order of magnitude greater than the emission from 300 nm excitation. Also, the slope of the 300 nm data is greater than that of the 340 nm data. The linear fit parameters are given in *Table 2*.

The fact that the data for both the uniaxially and biaxially deformed samples fall on the same line in *Figure 5* is an indication that planar extension is indeed a good measure of the orientation in this system. These results show that as far as trap fluorescence is concerned, biaxial and uniaxial stretching produce the same fluorescence behaviour (i.e. a 2×2 biaxial sample is comparable to a 4×1 uniaxial sample).

The PET film data of *Figure 5* may be explained by the following model, which is presented schematically in *Figure 6*. Excitation with 300 nm light directly excites monomer units in the chain backbone of the polymer. Immediate decay from the monomer produces an emission at 338 nm. In order to be emitted at 368 nm, however, one of two events must occur. One possibility is that the fluorescing structure, hereafter referred to as the trap, could be excited either by migration to the trap or by trivial absorption of the monomer emission at 338 nm. Once the trap is excited it fluoresces at 368 nm. If migration occurs, at each step in the energy migration route the energy could be lost in the form of monomer fluorescence or non-radiative decay, or the exciton could migrate to another unit, be it a monomer unit or a trap. From the observation that the 368 nm emission increases with increasing orientation, we conclude that increased orientation enhances energy migration to the trap. Such increased orientation increases the probability that at each step an exciton will migrate rather than decay, thus resulting in an increase in trap fluorescence. The trivial monomer emission–trap absorption process should not be affected by orientation. Thus, the amount of 368 nm emission resulting from trap absorption should be independent of planar extension.

The second possible mode of trap excitation is that it may be directly excited at 340 nm. Direct excitation is a much more efficient method of populating the trap when

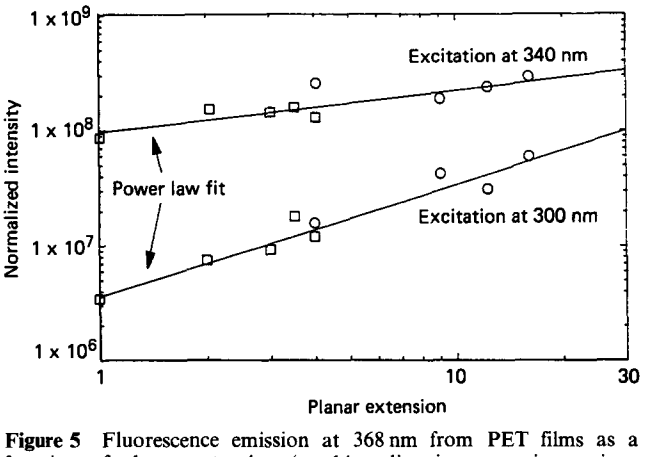

Figure 5 Fluorescence emission at 368 nm from PET films as a function of planar extension (machine direction extension ratio × transverse direction extension ratio) for excitation wavelengths of 300 nm and 340 nm. The intensity is normalized with respect to film thickness. □, Uniaxially deformed; ○, biaxially deformed

compared with energy migration. This explains why the 368 nm emission is much greater for excitation with 340 nm light than for excitation at 300 nm. The slight increase in 368 nm emission with film orientation for direct excitation may be due to increased trap formation upon deformation. Hennecke *et al.* found a small increase in the intrinsic fluorescence of uniaxially drawn samples with draw ratios from 2 to 5 (ref. 19). They attributed this to possible increase in trap (ground state dimer) concentration. Note that the model presented above does not depend in any way upon the specific structure of the trap. The subject of trap identification is dealt with below.

Differential scanning calorimetry

It is well known that stretching polymer films can cause stress induced crystallization. Thus, it is necessary to determine if the increase in fluorescence emission seen in *Figure 5* is somehow related to a commensurate change in sample crystallinity. D.s.c. scans were made on each of the oriented films in order to estimate relative amounts of amorphous and crystalline regions. A typical heating curve is given in *Figure 7*. Features which can be identified are a glass transition temperature (T_g) at 353 K, T_g overshoot at 355 K, recrystallization exotherm at 397 K and a melting endotherm at 527 K.

The area of a d.s.c. melting peak for a polymer is proportional to the crystalline content of that polymer. Similarly, the recrystallization peak area is proportional to the increase in crystalline content due to the thermal recrystallization process. In this study we are interested in relative changes in crystalline content with orientation rather than in absolute per cent crystallinities. Therefore, the following method was used to obtain the relative crystallinity in each film. It was found that the normalized melting peak area of each of the films was a constant to within 7%. This indicates that as each sample is heated it

Table 2 Linear fit parameters for *Figure 5*

	Excitation at	
	300 nm	340 nm
Slope	1.01	0.41
Linear intercept	15.13	18.44
Correlation coefficient	0.91	0.79

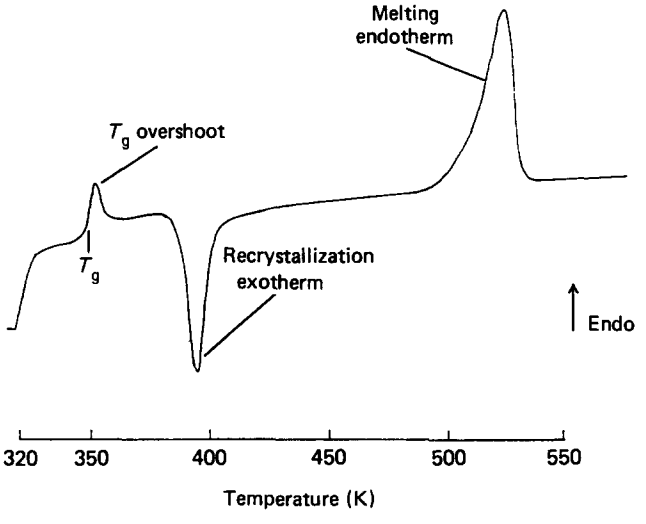

Figure 7 Typical d.s.c. heating curve for PET using a scan rate of 20 K min^{-1}

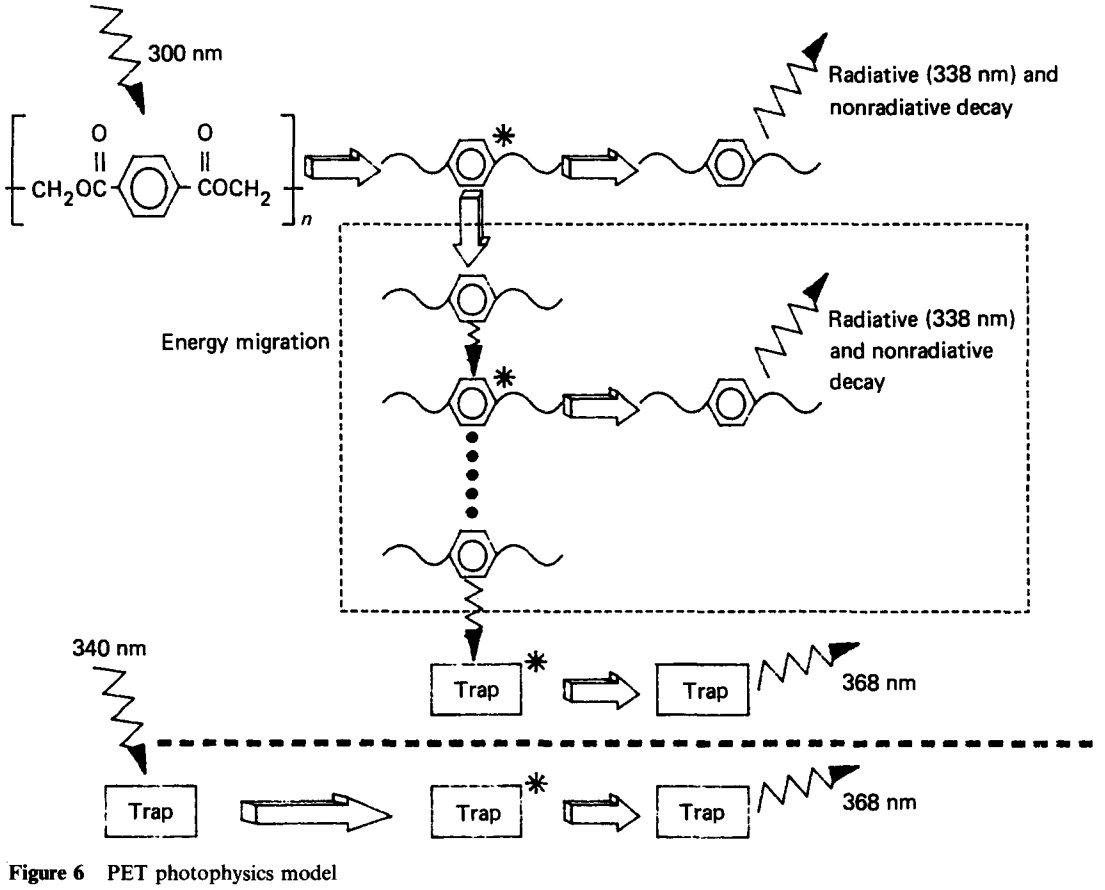

Figure 6 PET photophysics model

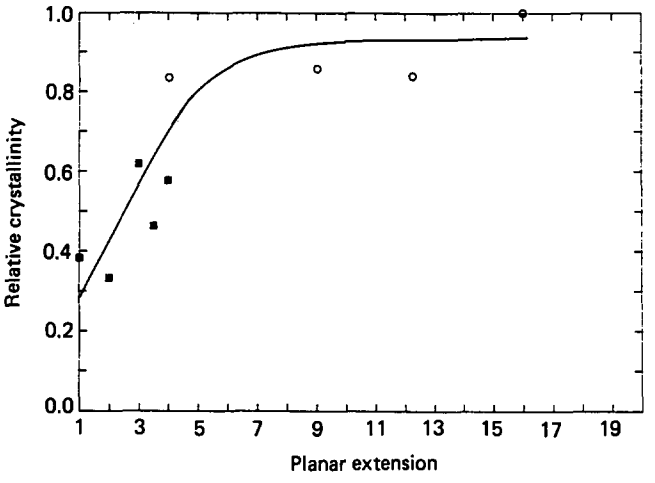

Figure 8 Relative crystallinity of PET films as a function of planar extension (machine direction extension ratio × transverse direction extension ratio). ■, Uniaxial extension; ○, biaxial extension

will recrystallize enough to raise the total crystalline content to this constant value, regardless of initial orientation. Thus, a number proportional to the initial crystalline content of each film can be obtained by subtracting the weight-normalized recrystallization peak area from the normalized melting peak area. Since we are only interested in the relative amounts of crystallinity, each value was normalized with respect to the value from the film with the largest planar extension. These results are plotted in *Figure 8*.

The d.s.c. results of *Figure 8* show that the relative crystallinity of the uniaxially stretched films increases with increasing extension. The biaxial samples show a higher amount of crystallinity, but the biaxial stretching produces less of a change in crystallinity than the uniaxial stretching. This finding is in general agreement with the behaviour observed by Heffelfinger *et al.*[21] and De Vries *et al.*[22]. These authors found that the initial effect of the uniaxial drawing was in the growth of crystallites, whereas the biaxial drawing mainly produced rotation and alignment of crystalline domains. This accounts for the rapid rise and then levelling off seen in *Figure 8*.

The variation in relative crystallinity may account for the small increase in 368 nm emission with planar extension using direct trap excitation of 340 nm seen in *Figure 5*. This does not necessarily mean that the traps are located in the crystalline regions, but it suggests that the morphological changes which produce a change in crystallinity may also cause a change in trap concentration. However, the stretched films do not differ enough in crystalline content to account for the large order of magnitude increase in 368 nm emission intensity with planar extension when using 300 nm excitation. This leads to the conclusion that energy migration from monomer units to the trap must occur in the amorphous regions surrounding the crystallite domains.

Padhye and Tamhane[15] have assigned the 368 nm emission band to a structure located in amorphous PET. They used plasma etching to observe the changes in PET fluorescence with changes in crystallinity. However, they used monomer excitation in their study, which means they were not observing fluorescence resulting from direct trap excitation. Therefore, since they were dramatically changing the amorphous phase of the films, they were most likely observing changes in the ease with which energy could migrate from monomer repeat units to the trap and not necessarily changes to the trap itself. Thus, their results seem to agree with the finding of this study that energy migration to the trap occurs in the amorphous regions.

These d.s.c. results show that the major effect that extension has on the films is not only the growth or formation of more crystallites, but may also be the ordering of the amorphous phase and aligning of crystallite regions. This conclusion is consistent with other published results[20-22].

Transient fluorescence

The above model proposes that in order for energy absorbed by a monomer unit to be emitted by a trap, the excitation must migrate to a trap. In general, this migration and subsequent emission should take longer than if a photon is directly absorbed by a trap and is then emitted. Therefore, transient fluorescence decay measurements should provide additional insight into these processes.

Fluorescence lifetime data for an unoriented PET film are shown in *Figure 9*. The decay profiles shown are for 368 nm emission using excitation wavelengths of 300 and 340 nm. The measured lamp profile used to deconvolute the raw data is also shown. The data were fitted to a multi-exponential equation using a modified Marquardt least-squares algorithm. Several statistical parameters were generated in order to analyse the goodness of fit. Single and double exponential trial functions did not result in an acceptable fit. A triple exponential, however,

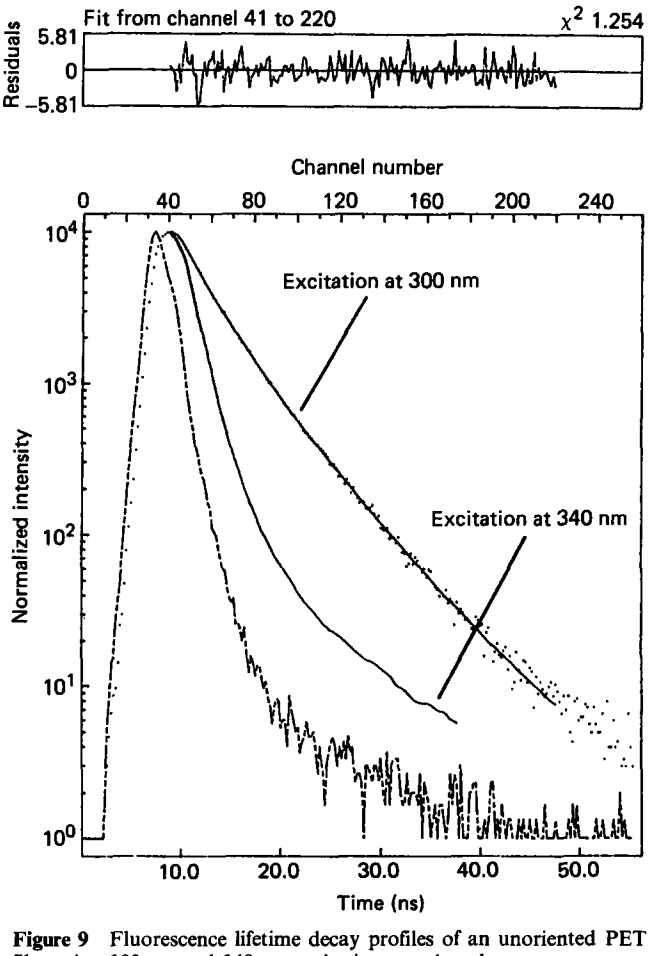

Figure 9 Fluorescence lifetime decay profiles of an unoriented PET film using 300 nm and 340 nm excitation wavelengths

Table 3 Transient fluorescence decay parameters
(a) Unoriented PET film: excitation wavelength = 300 nm, emission wavelength = 368 nm

Parameter				
Exp.	No.	Type	Parameter value	Parameter error
1	1	Ampl	0.46	0.04
	2	τ ns	0.78	0.13
		Int %	15.0	
2	3	Ampl	0.34	0.02
	4	τ ns	2.8	0.2
		Int %	40.4	
3	5	Ampl	0.19	0.02
	6	τ ns	5.6	0.1
		Int %	55.6	

$\tau_{ave} = 3.79$ ns

$\chi^2 = 1.25$
Durbin–Watson parameter = 1.76
Runs test parameter = 0.46

(b) Unoriented PET film: excitation wavelength = 340 nm, emission wavelength = 368 nm

Parameter				
Exp.	No.	Type	Parameter value	Parameter error
1	1	Ampl	1.39	0.01
	2	τ ns	0.99	0.02
		Int %	91.6	
2	3	Ampl	0.03	0.01
	4	τ ns	3.0	0.7
		Int %	6.5	
3	5	Ampl	0.003	0.002
	6	τ ns	9.1	2.3
		Int %	1.9	

$\tau_{ave} = 1.28$ ns

$\chi^2 = 1.34$
Durbin–Watson parameter = 2.05
Runs test parameter = 0.45

(c) 4 × 4 Oriented PET film excitation wavelength = 340 nm, emission wavelength = 368 nm

Parameter				
Exp.	No.	Type	Parameter value	Parameter error
1	1	Ampl	1.35	0.01
	2	τ ns	0.98	0.02
		Int %	88.3	
2	3	Ampl	0.05	0.02
	4	τ ns	2.7	0.5
		Int %	8.4	
3	5	Ampl	0.006	0.002
	6	τ ns	8.4	1.0
		Int %	3.3	

$\tau_{ave} = 1.37$ ns

$\chi^2 = 1.08$
Durbin–Watson parameter = 2.07
Runs test parameter = 0.23

did adequately reproduce the data. The statistics of each fit are presented in *Table 3*. The fitted lifetimes and corresponding pre-exponential factors are also given in *Table 3*. Note that the data were fitted from the data maximum to the channel after which the data are less than 0.1 % of the maximum.

The most striking feature of *Figure 9* is that the decay from excitation at 340 nm is faster than that for 300 nm excitation. This is in definite agreement with the proposed model, which predicts that 340 nm direct trap excitation should result in faster decay than decay after energy migration from a monomer unit.

The more quantitative aspects of the transient data should also be examined. For direct excitation at 340 nm, *Table 3* shows that the three exponential fit is dominated by the fast decaying component, since it produces over 91 % of the total integrated envelope area. The τ of this exponential is about 1 ns. This is in general agreement with the data of Hennecke and coworkers, which showed biexponential decay with the dominant lifetime being about 1.2 ns for 340 nm excitation of unoriented PET films[19].

In order to obtain a numerical comparison between the two decay profiles in *Figure 9*, a weighted average lifetime for each set of data was calculated. The weighting factor used in the computation was the fraction of the integrated area that each exponential contributed to the total. This method produced a τ_{ave} of 1.3 ns for direct trap excitation at 340 nm and a τ_{ave} of 3.8 ns for monomer excitation at 300 nm. It should be emphasized that these average 'lifetimes' are presented merely to show that direct trap excitation produces faster decay than monomer excitation and they do not necessarily represent any physically significant lifetimes.

The fact that three exponentials are required for a good fit indicates that there are complex photophysical processes taking place in this system. There is no evidence to support the idea that each of the three lifetimes carries some physical significance. In fact, since this system is three-dimensional in nature and energy migration occurs, complex, non-exponential behaviour can be expected[23]. Thus, it is not surprising that multiple exponentials are required to force a fit to this data.

Fluorescence decay profiles for a 4 × 4 biaxially oriented sample using 300 and 340 nm excitation were also measured. The three-exponential fit using 300 nm excitation is compared to the analogous data for an unoriented sample in *Figure 10*. This figure shows that the oriented sample decays slightly faster than the unoriented sample. This is in agreement with the proposed model. However, since the difference between the decay profiles is so small, a more quantitative comparison is not feasible. This may be another indication that the energy migration taking place in these oriented systems is not a simple process, especially in a biaxially ordered film.

The data for the direct excitation of the trap in the 4 × 4 film are also given in *Table 3*. The proposed model predicts that the decay from direct trap excitation should be essentially independent of sample orientation. This is indeed what the data of *Table 3* show. The τ values and pre-exponential factors of the oriented and unoriented films are comparable. Also, τ_{ave} of the oriented film (1.4 ns) is very close to that of the unoriented film (1.3 ns).

Fluorescence analysis of DMT and PET solutions

The above results and conclusions do not rely upon any assumptions about the structural characteristics of the trap. However, a more in-depth analysis of possible fluorescing structures could provide additional information about interactions, both electronic and physical, found in this system. Therefore, in order to

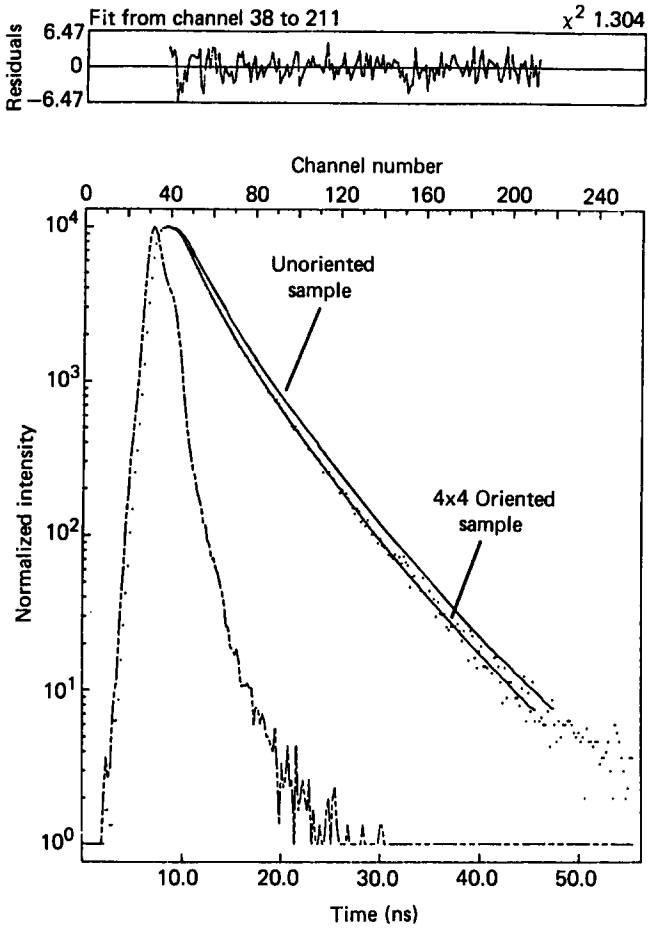

Figure 10 Fluorescence lifetime decay profiles of a 4 × 4 oriented and an unoriented PET film using 300 nm excitation

observe the fluorescence from more isolated PET chains, studies of PET in solutions of trifluoroacetic acid (TFAA) and dichloroacetic acid (DCAA) were conducted. These two solvents were chosen because DCAA is approximately a theta solvent for PET, whereas TFAA is a somewhat better solvent[24]. Thus, it was possible to observe the chains in solution under differing solvation conditions.

The solution behaviour of PET and DMT was observed by using monomer excitation at 300 nm and direct trap excitation at 340 nm. The emission spectra of PET and DMT solutions in TFAA and DCAA at a concentration of 2.6×10^{-4} molar repeat units and excited at 300 nm are shown in *Figure 11*. The solutions show a monomer emission band at about 325 nm, similar to the emission from DMT crystals shown in *Figure 2*. This monomer band is red-shifted to 338 nm in PET films (*Figure 4a*). Spectral red shifts are not uncommon when comparing the emission from crystalline solids and the corresponding solution data[25]. Note that in both solvents the emission from PET is weaker than that of DMT. This is probably the result of chain ends and branching impurities in the PET. Since the concentration of repeat units in PET was calculated by dividing a known weight of PET by the molecular weight of a repeat unit, the chain ends and any backbone impurities would cause the calculated concentration of repeat units to be higher than the actual concentration. Hence, the differences between PET and DMT in *Figure 11* are probably due to the fact that the actual concentration of emitting centres in the PET solutions was lower than in the DMT solutions. Another significant feature of *Figure 11* is that the emission from PET and DMT in DCAA is much weaker than in TFAA. That is most likely due to stronger quenching of the monomer emission in DCAA.

The concentration dependence of the 325 nm monomer emission is shown in *Figure 12*. Note that the data go through a maximum at a concentration of about 1×10^{-4} M. Also note that the observations from *Figure 11*, i.e. that the emission from DMT is stronger than PET emission in a given solvent and DCAA quenches more than TFAA, also hold for most concentrations in *Figure 12*. The maximum in the data can be explained as follows. At high concentrations the 325 nm emission is not seen due to self-absorption. However, as the concentration is decreased the molecules become more isolated and the emission intensity increases due to less self-absorption. If the concentration is further decreased, the intensity will

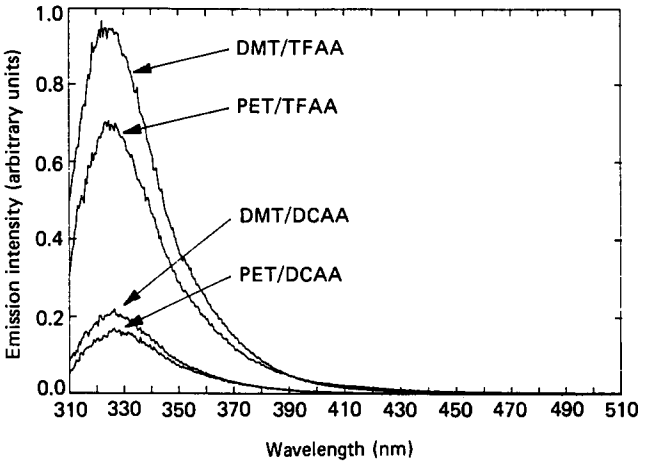

Figure 11 Fluorescence emission from PET and DMT solutions in DCAA and TFAA at a concentration of 2.6×10^{-4} M using an excitation of 300 nm

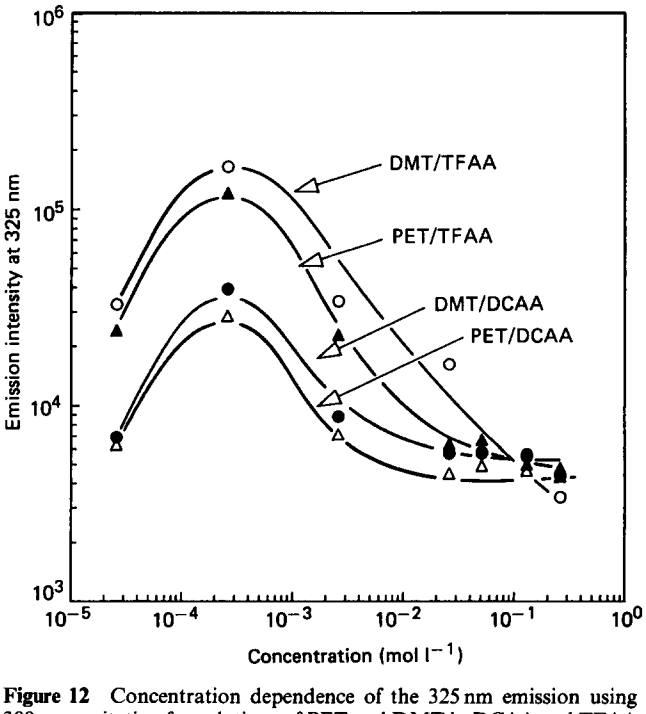

Figure 12 Concentration dependence of the 325 nm emission using 300 nm excitation for solutions of PET and DMT in DCAA and TFAA

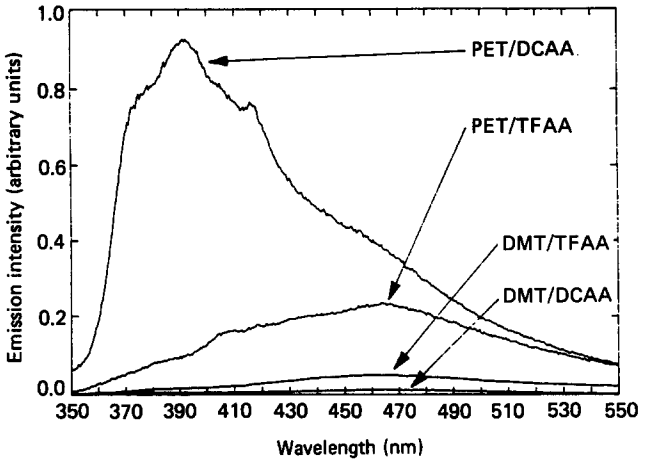

Figure 13 Fluorescence emission from PET and DMT solutions in DCAA and TFAA at a concentration of 0.26 M using an excitation of 340 nm

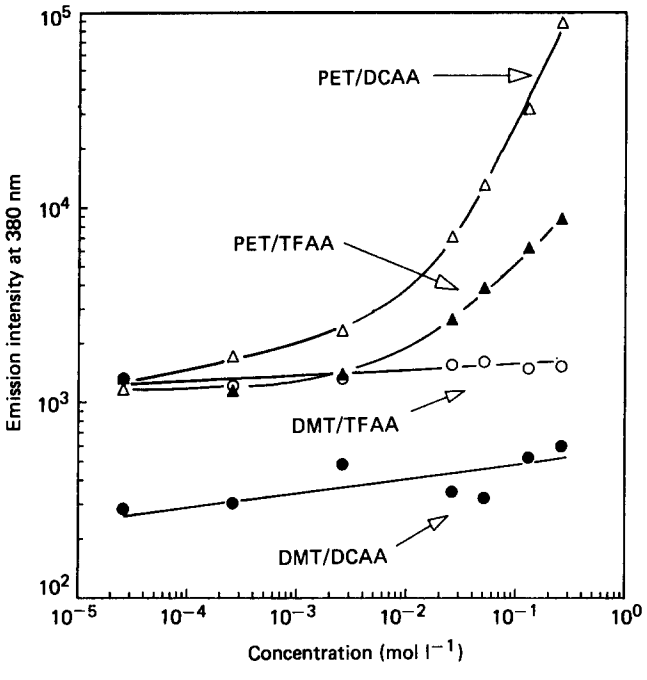

Figure 14 Concentration dependence of the emission at 380 nm from solutions of PET and DMT using 340 nm excitation

drop due to a decrease in chromophores, thus producing a maximum in the concentration *versus* intensity data.

The emission from PET and DMT solutions at a concentration of 0.26 molar repeat units using 340 nm direct trap excitation is given in *Figure 13*. A broad structureless emission from the DMT solutions can be seen. Note that, as with the monomer emission of *Figure 11*, the DCAA quenches the DMT emission more than the TFAA. A very different type of emission and quenching is observed from the PET solutions, however. The emission from PET in TFAA looks similar to that of the DMT solutions, only much stronger in intensity. However, the emission from PET in DCAA is radically different in intensity and band shape from the other solutions. This emission is similar to that of the PET film seen in *Figure 4b*.

The emission in the region of 450 to 460 nm is due to phosphorescence, possibly from the monomeric unit, since similar phosphorescence was observed in DMT crystals. A triplet emission at this wavelength has been observed by several authors[15-17]. However, Pacifici and Straley[26], and Day and Wiles[27] have found that an emission at 459 nm occurs for mono-hydroxylated PET, a product of photodegradation; unfortunately, no phosphorescence measurements were done on this emission. The possible emission from impurities is discussed further below. The similarity in band shape and the large difference in intensity between the PET in TFAA and the DMT solutions may indicate that the PET chains can inhibit some quenching of the phosphorescence by the solvent. Polymer coils may restrict access of the solvent molecules to the inner portions of the coil, thus decreasing the solvent's quenching ability, resulting in an increased emission.

The concentration dependence of the emission from these solutions is shown in *Figure 14*. Note that the DMT emission is relatively insensitive to concentration. By contrast, the PET emission is relatively constant up to about 1×10^{-2} M, at which point it increases with increasing concentration. The solvent exclusion and quenching arguments presented above may also explain this phenomenon; up to a concentration of about 1×10^{-2} M the emission is effectively quenched by the solvent. Above this concentration, the polymer chains hinder access by the solvent molecules.

DISCUSSION

Using the above solution and film data, some conclusions about the photophysical processes occurring in this system can be drawn. The structured excitation and emission spectra of *Figure 4b* for a PET film represent different vibrational transitions of the same fluorescing unit. That structure, and the fact that the monomer excitation spectrum (*Figure 2a*) is different from the polymer excitation spectrum of *Figure 4b*, lead to the conclusion that the emission from 360 nm to 420 nm cannot be from an excimer.

The differences in the emission of PET in solutions of TFAA and in solutions of DCAA give important information about possible interactions involved in the fluorescence. Comparison of *Figures 11* and *13* shows that when PET is in TFAA the emission is similar to that of the monomer model compound. On the other hand, PET in DCAA looks similar to the emission from PET films (*Figures 4b* and *13*). TFAA is a better solvent for PET than is DCAA. Therefore, in DCAA there will be more polymer–polymer interactions. Thus, it is not surprising that the emission for DCAA looks similar to that of the film, in which there is a high degree of polymer–polymer interactions. Similarly, in TFAA the chain experiences a higher degree of solvation and therefore reduced polymer–polymer interactions. It follows that the monomeric emission would be expected to dominate. This leads to the conclusion that the emission from the trap (from 360 nm to 420 nm) is strongly influenced by the degree of polymer–solvent interactions.

Note that direct excitation of the trap is seen in solutions of PET in DCAA (*Figure 13*). This solution behaviour gives valuable insight into the nature of the trap and its possible location. The fact that polymer–polymer interactions in solution produce trap

fluorescence lends support to the proposal that the trap may be an associated ground state dimer[17,18].

Since a solution most closely resembles the disordered nature of the amorphous phase of a polymer film, it would seem likely that the trap is located in the non-crystalline regions of the film. This is in agreement with the assignment by Padhye and Tamhane[15] of the 368 nm emission to a structure located in the amorphous regions of PET. The trap must also have an overlap configuration which is not found in the orthorhombic[28] crystalline domains of DMT, and is highly unfavourable in the DMT solutions. The small amount of fluorescence seen in the 360 nm to 400 nm region in DMT crystals may be due to traps found in the crystal defect regions. However, no energy migration to those traps is possible since no trap fluorescence was observed when exciting DMT crystals with 300 nm light. The fact that no trap emission is detectable when the monomer is excited in solutions of PET in DCAA shows that motions of the PET molecules in solution are occurring faster than migration can occur. In other words, an excited monomer in solution rarely 'sees' a trap to which it can transfer its energy.

These arguments, coupled with the d.s.c. results, seem to indicate that the migration is occurring in the non-crystalline phase, and thus the film extension produces some ordering of the non-crystalline regions. This is in agreement with the affine deformation model presented by Nobbs *et al.*[10-12] and supported by Hennecke *et al.*[18,19].

In all previous studies of the intrinsic fluorescence of PET[14-18], it was assumed that the emission in the 360 nm to 420 nm range was from the polymer and not due to an impurity of some kind. However, the possibility of impurity fluorescence must be addressed. In this study, PET samples from three independent sources were compared. All three had exactly the same structured emission in the 360 nm to 420 nm range. These results, combined with the similar emission noted in previous work[14-18], seem to indicate that if PET contains an impurity it is one that is commonly found in PET samples.

Two types of possible impurities should be considered. One is a small molecule that could be a remnant from the polymerization procedure. The other is an impurity in the chain backbone itself (e.g. a group attached to the backbone ring). Clearly the first type is not desirable in this study since fluorescence from it will not necessarily reflect true polymer backbone orientation. On the other hand, the latter type should not affect results to a great degree since the impurity is directly attached to the polymer backbone.

As a check for possible small molecule impurities, three Soxhlet extractions were performed on a PET film, and the fluorescence emission spectra of the film before and after each extraction were compared. Methanol, dichloromethane and hexane were used as extraction solvents in order to expose the film to various degrees of solvent polarity. The film was exposed to each solvent for 48 h. After each extraction the emission from the film was unchanged, leading to the conclusion that if an impurity is present in PET it is not of the small molecule form.

If branching takes place during PET synthesis, this could lead to a type of backbone impurity. More specifically, branches resulting from a free radical on a phenyl ring reacting with a backbone phenyl ring could lead to a biphenyl-like structure which would be fluorescent. It is beyond the scope of the present study, however, to delve into the details of the PET synthesis and any associated impurities arising from side reactions.

SUMMARY

The most significant general result of this study is that the intrinsic fluorescence of PET can be used as a probe of orientation in PET films. The orientation dependent fluorescence in the 360 nm to 420 nm range is from an unidentified trap structure located in the amorphous regions of the films. Energy migration, which is enhanced by uniaxial and biaxial orientation, can occur from monomer units to this trap. The experimental trapping results may be described by a power law relationship between trap fluorescence and planar extension. Stretching of these films produces increased ordering in non-crystalline regions and alignment of crystallite domains, with some increase in overall crystalline content. In contrast to the data obtained from polarized fluorescence and optical birefringence, the observable in this study changes by an order of magnitude over reasonable stretching ratios. Therefore, this technique appears to be more sensitive to orientation changes than other methods. The technique also appears to be applicable to both uniaxially and biaxially deformed samples.

ACKNOWLEDGEMENT

This work was supported by the Polymers Program of the National Science Foundation under Grant DMR 85-06669.

REFERENCES

1 Heffelfinger, C. J. and Lippert Jr, E. L. *J. Appl. Polym. Sci.* 1971, **15**, 2699
2 Purvis, J. and Bower, D. I. *J. Polym. Sci., Polym. Phys. Edn* 1976, **14**, 1461
3 Prevorsek, D. C., Kwon, Y. D. and Sharma, R. K. *J. Mater. Sci.* 1977, **12**, 2310
4 Pereira, J. R. C. and Porter, R. S. *Polymer* 1984, **25**, 869
5 Pereira, J. R. C. and Porter, R. S. *Polymer* 1984, **25**, 877
6 Casey, M. *Polymer* 1977, **18**, 1219
7 Rietsch, F., Duckett, R. A. and Ward, I. M. *Polymer* 1979, **20**, 1133
8 McGraw, G. E. *J. Polym. Sci. (A-2)* 1970, **8**, 1323
9 Bower, D. I., Korybut-Daszkiewicz, K. K. P. and Ward, I. M. *J. Appl. Polym. Sci.* 1983, **28**, 1195
10 Nobbs, J. H., Bower, D. I., Ward, I. M. and Patterson, D. *Polymer* 1974, **15**, 287
11 Nobbs, J. H., Bower, D. I. and Ward, I. M. *Polymer* 1976, **17**, 25
12 Nobbs, J. H., Bower, D. I. and Ward, I. M. *J. Polym. Sci., Polym. Phys. Edn* 1979, **17**, 259
13 Cunningham, A., Ward, I. M., Willis, H. A. and Zichy, V. *Polymer* 1974, **15**, 749
14 Phillips, D. H. and Schug, J. C. *J. Chem. Phys.* 1969, **50**, 3297
15 Padhye, M. R. and Tamhane, P. S. *Angew. Makromol. Chem.* 1978, **69**, 33
16 Takai, Y., Mizutani, T. and Masayuki, I. *Jpn. J. Appl. Phys.* 1978, **17**, 651

17 Allen, N. S. and McKellar, J. F. *Makromol. Chem.* 1978, **179**, 523
18 Hennecke, M. and Fuhrmann, J. *Makromol. Chem., Makromol. Symp.* 1986, **5**, 181
19 Hennecke, M., Kud, A., Kurz, K. and Fuhrmann, J. *Colloid. Polym. Sci.* 1987, **265**(8), 674
20 Jabarin, S. A. *Polym. Eng. Sci.* 1984, **24**, 376
21 Heffelfinger, C. J. and Schmidt, P. G. *J. Appl. Polym. Sci.* 1965, **9**, 2661
22 De Vries, A. J., Bonnebat, C. and Beautemps, J. *J. Polym. Sci., Polym. Symp.* 1977, **58**, 109
23 Fredrickson, G. H. and Frank, C. W. *Macromolecules* 1983, **16**, 572
24 Brandrup, J. and Immergut, E. H. (Eds) 'Polymer Handbook', Wiley, New York, 1975, p. V-77
25 Berlman, I. B. 'Energy Transfer Parameters of Aromatic Compounds', Academic Press, New York, 1973
26 Pacifici, J. G. and Straley, J. M. *J. Polym. Sci., Polym. Lett. Edn* 1969, **7**, 7
27 Day, M. and Wiles, D. M. *J. Appl. Polym. Sci.* 1972, **16**, 175
28 Brisse, F. and Perez, S. *Acta. Crystallogr.* (*B*) 1976, **32**, 2110